A Novel Bonding Method for Ionic Wafers

M. M. R. Howlader, Tadatomo Suga, and Moon J. Kim

***Abstract*—A novel method for bonding sapphire, $LiNbO_3$, quartz, and glass wafers with silicon using the modified surface activated bonding (SAB) method is described. In this method, the mating surfaces were cleaned and simultaneously coated with nano-adhesion Fe layers using a low energy argon ion beam. The optical images show that the entire area of the 4-in wafers of $LiNbO_3$/Si was bonded. Such images for other samples show particle induced voids across the interface. The average tensile strength for all of the mating pairs was much higher than 10 MPa. Prolonged irradiation reduced polarization in $LiNbO_3$, sapphire, quartz, and Al-silicate glasses. Fe and Ar ion-induced charge deposition result in the formation of an electric field, which was responsible for the depolarization. The lattice mismatch induced local strain was found in $LiNbO_3$/Si. No such strain was observed in the Al-silicate glass/Si interface probably because of annealing at 300 °C for 8 h. The Al-silicate glass/Si interface showed an interfacial layer of 2 nm thick. A 5-nm-thick amorphous layer was observed with the other layer across the $LiNbO_3$/Si interface. The EELS spectra confirmed the presence of nano-adhesion Fe layers across the interface. These Fe layers associated with the electric field induced by ion beam irradiation for prolonged period of time, particularly in $LiNbO_3$/Si, might be responsible for the high bonding strength between Si/ionic wafers at low temperatures.**

***Index Terms*—Auger electron spectroscopy, charge decomposition, depolarization, electron energy loss spectroscopy (EELS) and bonding strength, ionic wafers, lattice mismatch, modified hollow cathode ion source, polarization, surface activated bonding.**

I. Introduction

THE ionic materials are comprised of positive and negative ions, which are bound together by their electrostatic attraction. These materials spontaneously polarize at different polarization levels. Ionic materials such as $LiNbO_3$, sapphire, quartz, and glass have diverse applications in electronic, photonic, and micro-electro mechanical systems. Single crystalline $LiNbO_3$ is the material of interest for the fabrication of optoelectronic modulators, piezoelectric components, and microwave tunable devices [1]. The other material of interest is sapphire. With its wide transmission window, sapphire can improve bandwidth, reduce crosstalk, noise, and instability of CMOS optical receivers [2]. In addition, quartz, an optically transparent substrate, is considered as a candidate material for image sensors, displays, and optical waveguides [3]. Furthermore, the silicate glass is an inexpensive material compared with quartz, which is used for high frequency displays and those with a high pixel count [4]. Therefore, the bonding of these materials with single crystalline silicon can offer high-speed, high-bandwidth, and highly sensitive novel devices.

The wafer bonding technology enables the integration of different materials onto a single die. Wafer bonding techniques include direct wafer bonding, anodic bonding, eutectic bonding, thermal compression bonding, and temporary bonding. These techniques use high temperature, high voltage, high pressure, and specific composition to bond together diverse materials. A common challenge of these techniques is the bonding incapability of these materials due to lattice mismatch.

As alternatives to wafer bonding, few methods, which are crystal ion slicing [5], [6], chemical vapor deposition, radio frequency (RF) sputtering [7], and pulsed laser deposition, have been reported to combine these materials. The issues of how to improve the values of pyroelectric, electro-optic [1], and optical [6] properties of these films produced by these methods for such applications remain.

In order to get rid of these issues, we have developed a direct wafer bonding method at room temperature called the surface activated bonding (SAB) method. The SAB method joins two smooth, clean surfaces after removing contaminants, e.g., carbon and native oxides using an atom beam, ion beam, or plasma sources in a vacuum. The SAB method enables atomic level bonding, which produces interfaces with strengths equivalent to those of bulk materials. This technique has been implemented in the bonding of dissimilar metals to semiconductors to insulators at room temperature without heating and gluing. However, we have found difficulty in bonding ionic crystals with other materials using the normal SAB method.

The normal SAB failure in bonding ionic wafers is due to their inhomogeneous polarization after surface cleaning. To alleviate the adverse influence of polarization, we have modified the SAB method [8]. In this modified method, we have developed a modified hollow cathode ion source, capable of sputter cleaning and depositing thin Fe layers on the surfaces. This method allows prolonged sputter cleaning required for depolarization of ionic crystal surfaces. Also, it provides ultra-thin Fe layers, which keep the activated surfaces smooth and improve the refractive index, improving optical properties of ionic wafers such as $LiNbO_3$. Auger electron spectroscopy (AES) analysis is used to clarify the cleaning status and to detect the nano-adhesion layers on the surfaces. While the use of Fe as adhesion layers was intentional, similar results (not refractive index) can be achieved with nano-layers of Ti and Pd.

In this paper, we report the bonding between bare sapphire/silicon, $LiNbO_3$/silicon, quartz/silicon, and glass/silicon using the modified SAB method at low temperatures. In this method,

Manuscript received October 26, 2006; revised January 28, 2007. The work of M. M. R. Howlader was supported by the Ontario Photonic Consortium (OPC) at McMaster University.

M. M. R. Howlader is with the Engineering Physics Department and the Electrical and Computer Engineering Department, McMaster University, Hamilton, ON L8S 4K1, Canada (e-mail:mrhowlader@ece.mcmaster.ca.

T. Suga is with the Department of Precision Engineering, University of Tokyo, Tokyo 113-8656, Japan.

M. J. Kim is with the Department of Electrical Engineering, University of Texas at Dallas, Richardson, TX 75083 USA.

Color versions of one or more of the figures in this paper are available online at http://ieeexplore.ieee.org.

Digital Object Identifier 10.1109/TADVP.2007.906394

1521-3323/$25.00 © IEEE

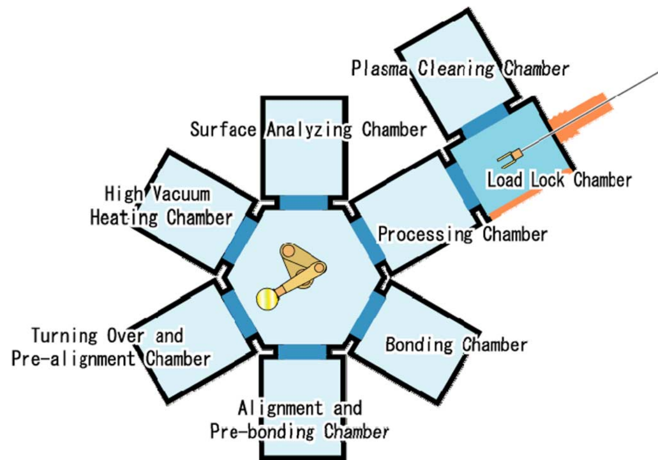

Fig. 1. Schematic diagram of surface activated bonding tool for wafer surface activation.

we utilize a modified low energy argon ion beam to remove surface contaminants and to deposit nano-adhesion Fe layers on the surfaces.

II. Experimental Procedure

A. Samples

A mirror-polished single crystalline (1102) sapphire wafer 50 mm in diameter, c-cut $LiNbO_3$ wafer 100 mm in diameter, quartz wafer 75 mm in diameter, amorphous Al-silicate glass wafer 125 mm in diameter, and (100) silicon wafer 200 mm in diameter were used for the bonding experiments. The thicknesses of the sapphire, $LiNbO_3$ quartz, glass, and Si wafers were 1000, 400, 375, 670 and 730 μm, respectively. The wafers were cleaned using the standard chemical cleaning procedure. An SAB tool scaled for the wafers was used for the experiments. The tool consists of eight chambers, the transfer chamber surrounded by processing, analyzing, heating, turning over/preliminary alignment (prealignment), alignment/preliminary bonding (prebonding), and bonding chambers, which all have pressure in the range 10^{-8}–10^{-9} torr (Fig. 1). A robot capable of handling 200-mm wafers is positioned in the transfer chamber, which has access to all chambers except the load lock.

B. Concurrent Surface Activation and Fe Deposition

A modified hollow cathode low energy Ar-ion beam source capable of etching at an incidence angle of 90° is located in the processing chamber. The ion source was modified in order to sputter deposit Fe with simultaneous sputter cleaning. As previously mentioned, the reason for Fe nano-layer deposition is to improve adhesion and raise the refractive index to improve optical properties of $LiNbO_3$, for example. The modification to the ion source was accomplished by covering an Fe ring on the hollow cathode surface. The accelerated ions in the discharged plasma have significant components in both the radial and axial directions. The radial ions may sputter Fe from the Fe ring surface and deposit it on the sample surface used for sputter cleaning [8].

The source can etch over a surface area of 200 mm in diameter. The wafers are rotated to achieve homogeneous etching during sputtering. The surface analysis chamber is equipped with an Auger electron spectroscopy, which accommodates 200-mm-diameter wafers. We have developed a wafer carrier, which normally carries 200-mm Si wafers, to carry 50-, 100-, and 125-mm diameter wafers. The wafers were loaded into the load lock chamber and kept there until the vacuum pressure reached 10^{-7} torr.

C. Surface Activation and Deposition Conditions

The wafers were sputtered separately in the processing chamber by a low energy argon ion beam with a voltage of 80 V and a current of 3 A. As mentioned earlier, the ion source sputter cleans and deposits Fe nano-adhesion layers simultaneously. The sputter cleaning times used for sapphire, $LiNbO_3$, quartz, glass, and Si were 22, 22, 30, 30, and 10 min, respectively. Sapphire, $LiNbO_3$, quartz, and glass and $LiNbO_3$ were first cleaned for 20 or 28 min (depending on the material), then cooled in a vacuum chamber, and finally cleaned for an additional 2 min.

Due to prolonged cleaning times to depolarize surface atoms with small amounts of nano-layer Fe, the temperature of the wafers increased to 200 °C within 5–10 min after starting sputtering. This increase was confirmed by measuring the temperature of the wafer by a thermocouple placed on the backside of the wafer. Without cooling the $LiNbO_3$, the bonding between Si and $LiNbO_3$ resulted in fractures in the bonded samples because of the CTE mismatch at 200 °C. Similar phenomena were observed in the bonding of Si with other combinations of ionic wafers. After cooling the wafers, the temperature significantly dropped. This resulted in no CTE effects at the bonded interface.

D. Bonding and Characterization

First, the activated (carbon removed and Fe deposited) Si wafer was transferred to the turning over and prealignment chamber, turned over, and transferred to the alignment and prebonding chamber. Second, the activated sapphire, $LiNbO_3$, quartz, and glass wafers were directly, but separately, transferred to the alignment and prebonding chamber after sputter cleaning. Finally, the activated (cleaned and Fe layers deposited) sapphire, $LiNbO_3$, quartz, and glass wafers were bonded together in the alignment and prebonding chamber under a load of 50 kgf.

The bonded wafers were cut into 10×10 mm^2 pieces and glued to metal bars for a tensile pulling test. Bonding strength was measured by a tensile pulling tester (AGS-1 kNG) from the Shimadzu Company. The bonded interfaces were investigated using a high-resolution transmission electron microscope (HRTEM).

III. Results

A. Auger Electron Spectroscopy for Surface Activation and Fe Deposition Analysis

The simultaneously cleaned and deposited surfaces are referred to as activated surfaces hereafter. In order to qualitatively investigate the activated surface, we used an AES. To avoid charging difficulty on oxide surfaces, we used silicon for the spectroscopy. Since silicon is a semiconductor and has no

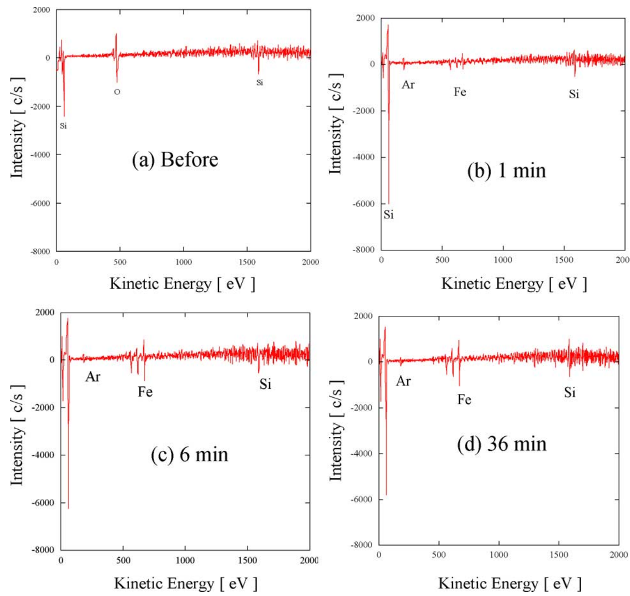

Fig. 2. AES of silicon surfaces before and after activation using modified low energy Ar-ion beam of 80 eV and 3 A. After activation, AES spectra for 1, 6, and 36 min treated samples were included. Ion beam allows surface cleaning and deposits Fe nano-adhesion layers on surface [8].

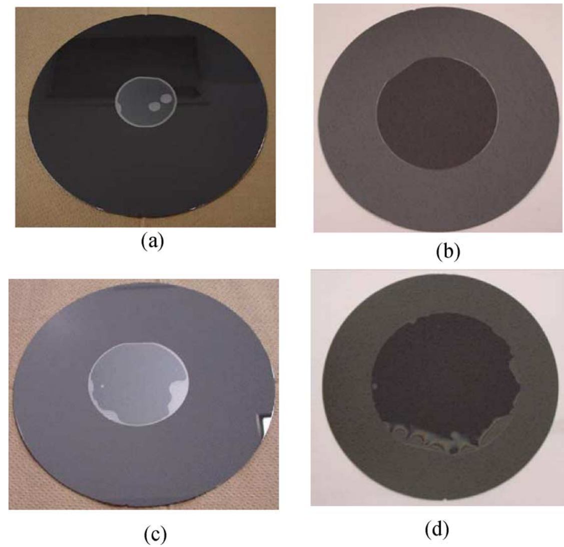

Fig. 3. Optical images of (a) sapphire/silicon, (b) $LiNbO_3$/silicon, (c) quartz/silicon, and (d) amorphous Al silicate glass/silicon wafers bonded in ultra-high vacuum pressure after activation with modified Ar-low energy ion beam at room temperature. Size of Si, sapphire, $LiNbO_3$, quartz, and glass wafers was 200, 50, 100, 75, and 125 mm, respectively.

charging problems with the energetic beam, the information for surface activation and back sputtering of Fe can be obtained. Although Si is different from oxide materials used in these experiments, we assume that the amounts of contaminants present on different surfaces are similar. The AES allows for the detection of the existence and influence of Fe deposition on the surfaces.

Fig. 2 shows the AES of silicon surfaces before and after sputter cleaning at 1, 6, and 36 min with the modified ion source. Before surface activation, native oxides are present on the surface. The contaminants such as carbon and native oxides disappeared after sputter cleaning for 1 min. The surface treated for 1 min showed a low amount of Fe on the surface. A low amount of Fe was detectable on the Si surface treated for 1 min and Fe counts remained constant with the increase of sputter cleaning time up to 36 min.

B. Optical Images of Interfaces

Fig. 3 shows the optical images of sapphire/silicon, $LiNbO_3$/silicon, quartz/silicon, and glass/silicon interfaces bonded by the modified SAB method at room temperature. The sputter cleaning and deposition times for sapphire, $LiNbO_3$, quartz, glass, and Si were 22, 22, 30, 30, and 10 min, respectively. The size of sapphire, $LiNbO_3$, quartz, glass, and Si were 50, 100, 75, 125, and 200 mm, respectively. The Fe layer thickness for the 22-min activated Si surface was 2 nm. An ellipsometer (HS-190) from J. A. Woollam Co., Ltd., was used for the Fe layer thickness measurement.

The optical images of different bonded interfaces show dissimilar behavior. For example, two void regions are found across the interface of sapphire/silicon, whereas the entire area of $LiNbO_3$/silicon is bonded. While the characteristic behaviors of bonded interfaces were reproducible, the numbers of voids varied across the interfaces.

On the other hand, unbonded areas were found across the peripheral regions of quart/silicon and glass/silicon wafers. Therefore, the unbonded characteristics can be classified into two groups: peripheral and nonperipheral. Surface scratches by tweezers while holding the wafer and wafer warpage can be attributed to the voids at the unbonded peripheral areas. If the wafer warpage is more than 6 μm over 8 in, the water molecules from the controlled atmospheric air after deloading the bonded sample accumulated in the open region in the interfaces, causing warpage.

Since the wafers were handled in a 10 000-class clean room, we assume that the nonperipheral void area is generated due to the particles left on the activated surfaces.

C. Tensile Strength

The bonded wafers were cut into $10 \times 10\text{-mm}^2$ pieces and glued to metal bars (jigs) for the tensile pulling test. The tensile tester attempted to separate the bonded wafers by pulling metal bars adhered to the bonded wafers in two opposite directions perpendicular to the bonded surfaces. The tensile pulling speed was 1 mm/min, which was computer controlled, as was the data acquisition.

The tensile pulling test results for sapphire/Si and $LiNbO_3$/Si bonded wafers with transparent Fe layers, including bonding and annealing conditions, are shown in Table I. The respective bonding strengths were in the range as of 6.8–13.5, 8–37.5, 6–14.4, and 15–45.2 MPa. The numbers of samples randomly picked for sapphire/Si, $LiNbO_3$/Si, quartz/Si, and glass/Si pairs were 9, 31, 12, and 40, respectively. The broad range of bonding strength may be due to different inclusions such as dust/particles at the interface, inhomogeneous force application to the surfaces due to parallelism problem of the jigs and their angle during pulling test, and inhomogeneous plasma etching of the surface, etc. [9]. The average tensile bonding strength for each pair of bonded samples was higher than 12 MPa. The majority of the

TABLE I
TENSILE RESULTS OF SAPPHIRE/SI, $LiNbO_3(LN)$/SI, QUARTZ/SI, AND AL SILICATE GLASS/SI WAFERS BONDED WITH TRANSPARENT FE LAYERS AT ROOM TEMPERATURE. QUARTZ/SI AND AL SILICATE GLASS/SI PAIRS WERE ANNEALED IN AIR AT 300 °C

Mating wafers	Activation time [min]	Bonding temperature	Post-bonding heating	Bonding strength [MPa]
Al_2O_3/Si	22/10	RT	-	6.8-13.5
LN/Si	22/10	RT	-	8-37.5
Quartz/Si	30/10	RT	300°C	6-14.4
Si/glass	30/10	RT	300°C	15-45.2

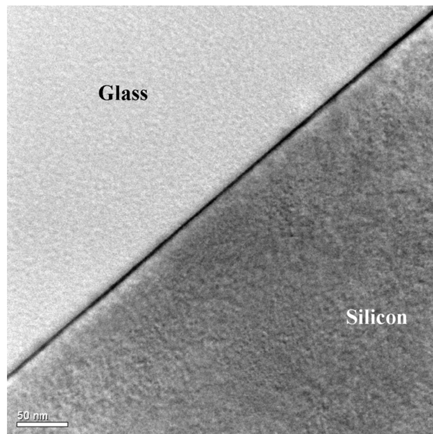

(a)

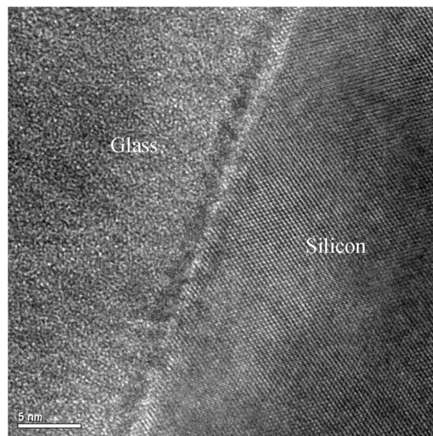

(b)

Fig. 4. (a) Low resolution and (b) high resolution TEM images for Al-silicate glass/Si heated at 300 °C. Bonded sample was heated to enhance bonding strength.

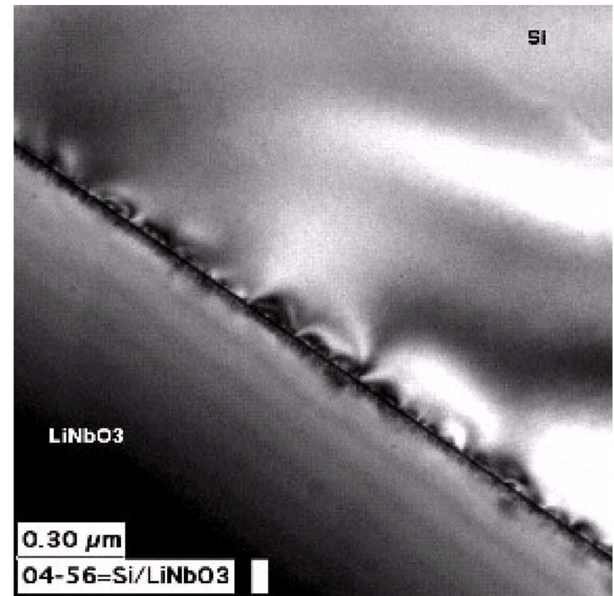

(a)

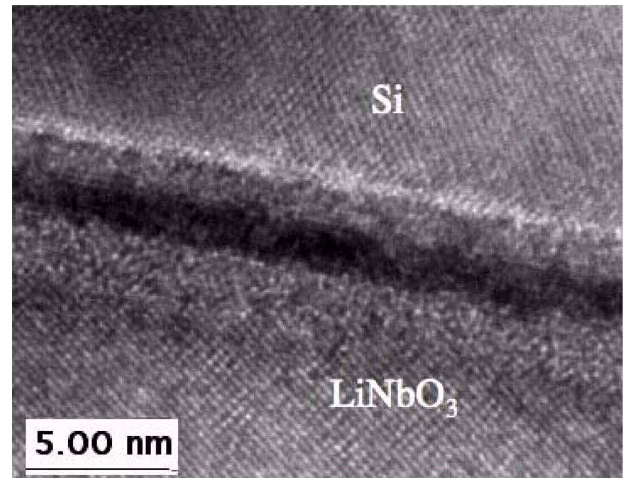

(b)

Fig. 5. TEM images with (a) low magnification and (b) high magnification for $LiNbO_3$/Si bonded at room temperature. Sample was not heated after bonding. Amorphous layer with dark crystalline Fe layer is observed across the interface. Observed lattice fringes are not as sharp as they should be because crystal tilt for HRTEM imaging was optimized to mediate a slight rotational misorientation of bonded $LiNbO_3$/Si pair.

samples fractured from the bulk materials and showed excellent bonding strength. The other samples that fractured at the glue and interface showed tensile strengths below 10 MPa.

Sapphire/Si and $LiNbO_3$/Si bonded wafers were not heated because of their adequate bonding strengths. Whereas quartz/Si and glass/Si wafers were heated at 300 °C for 8 h in air to increase their bond strengths. These bonded pairs were delaminated during dicing into chips.

D. Microstructure Observation of Interfaces

Fig. 4 shows the low- and high-resolution (HR) transmission electron microscopy (TEM) images of Al-silicate glass/Si heated at 300 °C at room temperature after bonding. The activation time for glass and Si was 30 and 10 min, respectively. The low magnification images showed an interface free from strain and defects. Thermal annealing may improve localized strain. The HRTEM image showed a layer, presumably containing deposited Fe, of about 2 nm thick between the crystalline Si and amorphous silicate glass interface.

Fig. 5(a) shows a low-magnification image for $LiNbO_3$/Si bonded at room temperature. The image shows periodic shading due to the local strain between the two lattice sites [10]. Fig. 5(b) shows the HRTEM image of the $LiNbO_3$/Si bonded interface. The observed lattice fringes are as sharp as they could be because the crystal tilt for HRTEM imaging was optimized to mediate a slight rotational misorientation of the

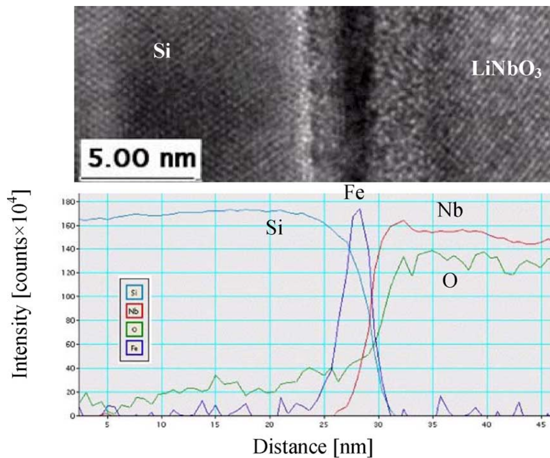

Fig. 6. Compositional distribution by EELS analysis across $LiNbO_3$/Si interface. Upper left and upper right (red) lines show Si and Nb, respectively [12]. Center of interface is near crossing of these two curves. Fe curve is across center, which looks like a Gaussian curve. Left and right sides from center represent Si and $LiNbO_3$ wafers, respectively. Horizontal and vertical axes represent distance across interface in nanometers and signal counts $\times 10^4$, respectively. Spatial resolution of analysis shown is about 1 nm.

bonded $LiNbO_3$/Si. An amorphous layer of 5 nm was observed across the interface. A dark contrast region, probably crystalline Fe, was found across the interface. In order to investigate the elemental distribution across the bonded interface, an electron energy loss spectroscopy (EELS) analysis was carried out.

E. EELS for Fe Investigation

Fig. 6 shows the longitudinal EELS analysis for elemental distribution across the Si/$LiNbO_3$ interface corresponding to the bonded interface shown by HRTEM. Fe is shown to be at its highest concentration at the center of the interface. Its amount decreases as it moves into the bulk materials both on the Si (left) and $LiNbO_3$ (right) sides. At the intersection of Si and Nb curves (that apparently is at the center of the interface), little Fe is found on $LiNbO_3$ compared with Si. However, the irradiation time for the $LiNbO_3$ wafer was 22 min, whereas the irradiation time for Si was 10 min. Thus, the thickness of Fe on $LiNbO_3$ should be higher than that of Si. This might correspond to the lower projected range and implantation [11] of Ar and Fe in $LiNbO_3$ than those in Si. The EELS spectra showed lower Fe implantation/occupation in the lattice sites of $LiNbO_3$. Damage accumulation may be due to the randomly incorporated Ar and Fe. Heating effects may also be due to the implanted Ar and Fe ions in the wafers.

IV. Discussion

A. Polarization and Depolarization

After an extensive investigation of the activation time dependence on the bonding of ionic crystals with Si, we have carefully chosen the activation time for ionic wafers. The activation time for Si was not detrimental to the bonding with sapphire, $LiNbO_3$, quartz, and glass. However, if the activation time was less than 20 min for $LiNbO_3$ and 30 min for quartz, and glass, Si did not bond with these wafers.

The AES study of the Si surface showed that the time to remove the contaminants and native oxides from these materials ranged from a few seconds to several minutes. Also, the surface cleaning does not significantly increase Fe layers on the surfaces after a 6-min activation period. Furthermore, the Si/Si wafers were bonded after 30–60 s of activation. The facts indicate that longer activated times of these samples than that of Si is intrinsically related to the material properties. This intrinsic nature could be the surface polarization of these ionic wafers.

As previously mentioned, the sputter cleaned and Fe nanolayer coated ionic wafers were not bonded unless treated for about 20 min. While the thickness of deposited Fe layers become constant after 6–10 min, the extra discrepant time (10–20 min) required for the activation of $LiNbO_3$ and sapphire is indicative of the dominant influence of polarization over bonding more than Fe layers deposition.

We will concentrate only on $LiNbO_3$ to understand the polarization criterion of $LiNbO_3$, which occurs due to surface structure change after treatment by energetic sources. In general, the position shift of lithium and niobium cations in the same direction relative to the oxygen plane rises to the polarity of that of a crystal. When Ar-ion plasma hits the targeted surface of $LiNbO_3$, solid-state reactions such as etching of surface elements, e.g., Li, Nb, and O, and implantation [11], [12] of a certain amount of Ar ions are expected. These physical processes increase the temperature and induce an electric field in the sample. The Auger analysis of the silicon surface showed the presence of Ar-ions after activation. In addition, we detected an increase of sample temperature to as high as 473 K during activation. We note that the samples to be sputtered clean were placed on metallic plates, which served as the ground.

The RF plasma [13], electron beam [14], and electric field [15] are generally used for modification of the surface of $LiNbO_3$ for waveguide applications. These processes have been reported to inverse domain and reduce polarization of $LiNbO_3$ [13]–[15]. The charge deposited by a plasma and electron beam neutralizes the polarization, resulting in depolarized activated surfaces. Therefore, we believe that the electric field generated by the charge deposition due to the activation for a long time neutralizes polarization in $LiNbO_3$ and other ionic materials.

B. Bonding Mechanism

The Fe nano-adhesion layer deposition and depolarization are two independent mechanisms that contribute to adhesion enhancement of the ionic wafers bonded with Si. It is almost impossible to distinguish separate roles of these two parameters on the bonding of ionic wafers.

Recently, the sputter cleaning time for Si/Si bonding was reported to be 30 s because there is no concern of polarization in Si wafers. The ionic wafers were not bonded with Si without Fe nano-adhesion layers. Surface adhesion layers were needed to produce adhesion between Si/Al silicate glass and quartz/quartz wafers. The modified Ar-ion source was used for sputter cleaning with simultaneous Fe deposition [8], [12].

The EELS measurements showed Gaussian distribution of Fe across the interface. Enhancing strength of Si/Al silicate glass and Si/quartz by heating may indicate rearrangement of Fe with

host atoms. Prolonged sputter cleaning with nano-layers Fe deposition may depolarize and smooth the mating surfaces. Subsequent bonding may induce strong adhesion by cross-linking Fe on mated depolarized surfaces.

V. Conclusion

We have bonded sapphire/Si, $LiNbO_3$/Si, quartz/Si, and silicate glass/Si wafers using a modified surface activated bonding (SAB) process at room temperature. A low energy argon ion beam of 80-eV energy with 3-A current was used, which was capable of sputter cleaning and depositing Fe nanolayers on the surfaces. The Auger electron spectroscopy showed Fe and Ar ions on the activated surfaces. The optical images showed that the entire area of 4-in wafers of $LiNbO_3$/Si was bonded. Such images for other samples showed particle-induced voids across the interfaces. The average tensile strength for all of the mating pairs was much higher than 10 MPa.

The prolonged irradiation reduced polarization in $LiNbO_3$, sapphire, quartz, and Al-silicate glasses. Fe and Ar ions induced a charge deposition probably resulting in the electric field, which was responsible for the depolarization. The lattice mismatch-induced local strain was found in $LiNbO_3$/Si. No such lattice strain was observed in the Al-silicate glass/Si interfaces probably because of annealing at 573 K for 8 h. The Al-silicate glass/Si interface showed a new 2-nm-thick layer. An amorphous layer 5 nm thick was observed with a dark layer across the $LiNbO_3$/Si interface. The EELS spectra confirmed the presence of nano-adhesion Fe layers across the interface. These Fe layers associated with the electric field induced by ion beam irradiation for a long time, particularly in Si/$LiNbO_3$, might be responsible for the high bonding strength between Si/ionic wafers at low temperature.

References

[1] G. Griffel, S. Ruschin, and N. Croitoru, "Linear electric-optic effect in sputtered polycrystalline $LiNbO_3$ films," *Appl. Phys. Lett.*, vol. 54, no. 15, pp. 1385–1387, 1989.

[2] J. J. Liu, Z. Kalayjian, B. Riely, W. Chang, G. J. Simonis, A. Apsel, and A. Andreou, "Multichannel ultrathin silicon-on-sapphire optical interconnects," *IEEE J. Select. Topics Quantum Electron.*, vol. 9, no. 2, pp. 380–286, Feb. 2003.

[3] Q.-Y. Tong and U. Gosele, *Semiconductor Wafer Bonding: Science and Technology*. New York: Wiley, 1999.

[4] M. J. Wild, A. Gillner, and R. Poprawe, "Locally selective bonding of silicon and glass with laser," *Sens. Actuators A*, vol. 93, pp. 63–69, 2001.

[5] M. Cai, D. Qiao, L. S. Yu, S. S. Lau, C. P. Li, L. S. Hung, T. E. Haynes, K. Henttinen, I. Suni, V. C. M. Poon, T. Marek, and J. W. Mayer, "Single crystal Si layers on glass formed by ion cutting," *J. Appl. Phys.*, vol. 92, no. 6, pp. 3388–3392, 2002.

[6] M. Levy, R. M. Osgood Jr., R. Liu, L. E. Cross, G. S. Cargill , III, A. Kumar, and H. Bakhru, "Fabrication of single-crystal lithium niobate films by crystal ion slicing," *Appl. Phys. Lett.*, vol. 73, no. 16, pp. 2293–2295, 1998.

[7] T. A. Rost, H. Lin, T. A. Rabson, R. C. Baumann, and D. L. Callahan, "Deposition and analysis of lithium niobate and other niobium oxides by RF magnetron sputtering," *J. Appl. Phys.*, vol. 72, no. 9, pp. 4336–4343, 1992.

[8] M. M. R. Howalder, H. Okada, T. H. Kim, T. Itoh, and T. Suga, "Wafer level surface activated bonding tool for MEMS packaging," *J. Electrochem. Soc.*, vol. 151, no. 7, pp. G461–G467, 2004.

[9] M. M. R. Howlader, S. Suehara, H. Takagi, T. H. Kim, R. Maeda, and T. Suga, "Room-temperature microfluidics packaging using sequential plasma activation process," *IEEE Trans. Adv. Packag.*, vol. 29, no. 2, pp. 448–456, Feb. 2006.

[10] Y. Tomita, M. Sugimoto, and K. Eda, "Direct bonding of $LiNbO_3$ single crystals for optical waveguides," *Appl. Phys. Lett.*, vol. 66, no. 12, pp. 1484–1485, 1995.

[11] C. J. McHargue, "Ion beam modification of ceramics," *Mater. Sci. Technol. A*, vol. 253, pp. 94–105, 1998.

[12] M. M. R. Howlader, T. Suga, and M. J. Kim, "Room temperature bonding of silicon and lithium niobate," *Appl. Phys. Lett.*, vol. 89, pp. 031914–3, 2006.

[13] H. Turcicova, J. Zemeck, J. Vacik, J. Cervena, V. Perina, M. Polcarova, and J. Bradler, "Surface analysis of $LiNbO_3$ single crystals modified by radio-frequency hydrogen plasma," *Surf. Inter. Anal.*, vol. 29, pp. 260–264, 2000.

[14] M. Fujimura, K. Kinataka, T. Suhara, and H. Nishihara, "$LiNbO_3$ waveguide quasi-phase-matching second harmonic generation devices with ferroelectric-domain-inverted gratings formed by electron-beam scanning," *J. Lightwave Technol.*, vol. 11, pp. 1360–1368, Nov. 1993.

[15] K. Kinataka, M. Fujimura, T. Suhara, and H. Nishihara, "Fabrication of ferroelectric-domain-inverted in $LiNbO_3$ by applying voltage using etched-Si-stamper electrode," *Electron. Lett.*, vol. 34, no. 9, pp. 880–881, 1998.

M. M. R. Howlader received the B.Sc.Eng. degree in electrical and electronic engineering from Khulna University of Engineering and Technology, Khulna, Bangladesh, in 1988, and the M.S. and Ph.D. degrees in applied quantum physics and nuclear engineering from Kyushu University, Fukuoka, Japan, in 1996 and 1999, respectively.

He was a Postdoctoral Scholar at the University of California, Davis, in 1999, and worked on radiation effects on materials. From 2000 to 2005, he was with the Research Center for Advanced Science and Technology, University of Tokyo, Tokyo, Japan, as a member of faculty, where he was an endowed Associate Professor with the center. He is currently with the Engineering Physics Department and Electrical and Computer Engineering Department, McMaster University, Hamilton, ON, Canada. He has published 23 technical papers and over 50 international proceeding articles. His research interests include the nano-bonding of dissimilar materials and individual wafers, components and elements from emerging technologies of microelectronic, optical, chemical, micro electromechanical systems (MEMS), and BioMEMS to create miniaturized and robust systems, oxidation behavior of solders and electronic materials, interfacial adhesions, and radiation effects on materials and packages.

Dr. Howlader is a member of Japan Institute of Electronic Packaging (JIEP) and he received the Best Technical Paper Award at the International Conference on Electronic Packaging in 2003.

Tadatomo Suga received the M.S. degree in precision engineering from the University of Tokyo, Tokyo, Japan, in 1979. He received the Ph.D. degree from the University of Stuttgart in 1983 for his study on fracture mechanics characterization of metal-ceramic interfaces.

In 1984, he became a member of the Faculty of Engineering, the University of Tokyo, and since 1993, he has been a Professor of Precision Engineering. He is Director of a research group at the National Institute of Materials Science (NIMS). His research interests include micro-systems integration and packaging, and development of interconnect technology, especially the room temperature bonding technique for various applications. He has endeavored to establish collaboration between industries and academia for the packaging technology. He organized the foundation of the Institute of Micro-System Integration (IMSI) in 1997, the first consortium for the competitive packaging industry which consists of 30 Japanese companies. He has published 200 papers and five books in the field of material science and electronic packaging.

Dr. Suga has advocated the importance of environmental aspects of packaging technology and is well known as the key organizer of Japanese roadmap of lead-free soldering and International Eco-design Conference. He was appointed as the 20th council member of the Japan Council of Science, October 2005.

Moon J. Kim received the B.S., M.S., and Ph.D. degrees in materials science and engineering from Arizona State University, Tucson.

He is a Professor in the Department of Electrical Engineering at the University of Texas, Dallas, and is also the Director of the Nano-Characterization Facility. His expertise ranges from high resolution electron microscopy to heterogeneous materials integration by wafer bonding. His current research interests include advanced Si-CMOS, nano-electronics, nano-bio technology. He has conducted extensive interdisciplinary materials research involving state-of-the-art HREM and has designed and built a unique ultra high vacuum (UHV) wafer bonding unit. He has authored/co-authored more than 145 refereed papers and given more than 45 invited talks.